QUANTUM MONTE CARLO FOR REALISTIC AND MODEL SOLIDS

PAOLA GORI-GIORGI, ALESSANDRO FEDERICO, AND GIOVANNI B. BACHELET

Dipartimento di Fisica, Unità INFM and CASPUR, Università di Roma "La Sapienza", Piazzale A. Moro 2, 00185 Rome, Italy

1 Introduction

By far most papers of this symposium are devoted to atoms, molecules and clusters. Only very few deal, one way or another, with extended systems. After very briefly listing some achievements and open problems on realistic solids (on which a good review was recently published[1] and a few results appear elsewhere in this volume), we plan to illustrate the role of QMC simulations for two popular model solids: the two-dimensional (2D) Hubbard hamiltonian, and the three-dimensional (3D) homogeneous electron gas, or jellium. Both models are of great interest to the chemistry and physics of solids, although neither one is directly related to any particular, real compound.

1.1 Realistic solids

Structural properties, interatomic forces and charge densities of many realistic solids are well described by the density functional theory[2,3,4] with a local-density approximation (LDA) for its exchange-correlation energy functional. Generalized gradient approximations (GGA)[5] seem to provide a good description even for some chemical bonds, like the hydrogen bond, for which the LDA is not adequate. The effective replacement of atomic cores by nonlocal pseudopotentials[6], the unified approach to density functional theory and molecular dynamics[7], and the linear response theory[8], have evolved into a set of well-established, standard tools,[9] by which not only static and vibrational properties of solids, but even the dynamics of liquids and some catalytic reactions may be attacked[10]. If approximate density functionals and single-particle Bloch orbitals work so well for infinite periodic systems, why should one embark in QMC simulations and deal with much less comfortable many-electron wavefunctions and finite-size samples? One reason to do so is that the best-to-date density functionals still miss key qualitative aspects of rather interesting solids, like e.g. the low-temperature phases of high-Tc superconductors or the room-temperature static properties of plutonium;[11] QMC could help understand strong electron correlations in such real materials. On a finer scale, another reason to embark in QMC simulations is a better quantitative understanding of electron correlations in simple (say, s-p) compounds,[12] possibly with a feedback on density-functional theory.[13]

1.2 Pseudopotentials, fixed nodes and forces

For both types of solids it turns out that pseudopotentials are absolutely necessary for QMC simulations, since the multiplicity of energy and spatial scales typical of the inner-shell structure of atoms makes atoms heavier than neon practically intractable; apart from the mathematical problem of turning their inherent nonlocality into some equivalent local operator (needed by projection MC techniques)[1,14], there is a more serious problem related to the physics of strongly nonlocal ions, like d- or f-metals, for which (apart from the obvious but costly idea of promoting shallow core shells into the family of valence electrons) a satisfactory pseudopotential scheme has yet to be found.[15]

Another aspect common to all projection MC techniques is the fixed-node approximation, on which active research is underway[16]. This is especially critical for large and strongly correlated extended systems, for which a good guess of the nodal structure cannot be expected from approximate single-particle schemes.

1.3 Model solids

As a result, while progress on better optimization schemes of the trial function[1,12] and even preliminary studies on interatomic forces[17] are underway for a wealth of interesting s-p solids, QMC simulations of strongly correlated systems are, for the time being, limited to simple model hamiltonians. For them QMC simulations are hard but feasible, and may provide complementary information with respect to other theoretical approaches. As an example we recall, in what folllows, some recent results on phase separation in the two-dimensional Hubbard model.

Another simple hamiltonian which for different reasons is of relevance to solid-state physics and has been the object of extensive QMC simulations is the jellium model. Neglecting its intrinsic strong-correlation regime (very low densities), we will here concentrate on the feedback of these simulations, in the medium- and high-density regime, into the progress of density functional theory.

2 Two-dimensional Hubbard model

2.1 Background

Strongly correlated electrons and holes are expected to play a key role in the high-T_c superconductors. Their possible instability towards phase separation, initially believed to inhibit superconductivity, gained special interest when different authors [18,19] pointed out that it could, in fact, favor it. Phase-separation and/or charge instabilities (e.g. incommensurate charge-density waves or stripes) are related to a substantial reduction of the kinetic energy, which otherwise tends to stabilize uniformly distributed states, which is typical of (real and model) strongly correlated electrons.

2.2 Phase separation

Phase separation is a thermodynamic instability associated to the violation of the stability condition $\chi^{-1} = \partial^2\mathcal{E}/\partial n^2 > 0$, which requires the energy density $\mathcal{E}$ of an infinite electronic system to be a convex function of the electron density n. If it occurs in the density range $n_1 < n < n_2$, then the system will separate into two subsystems with electron densities n_1 and n_2. For the two-dimensional single-band Hubbard hamiltonian

$$\mathcal{H} = -t \sum_{\langle i,j\rangle\sigma} (c^\dagger_{i\sigma} c_{j\sigma} + h.c.) + U \sum_i n_{i\uparrow} n_{i\downarrow}, \tag{1}$$

which is supposed to catch the main physics of electrons near the Fermi energy in the copper-oxygen planes of high-T_c materials, a phase separation, if any, is expected to occur in a density range close to half filling ($n \simeq 1$), and to yield a hole-rich phase with electron density $n_1 < 1$ and a hole-free phase with electron density $n_2 = 1$, in analogy with the behavior of a related toy hamiltonian, the t-J model[20]. This could be due to the great stability of the half-filling ($n = 1$), insulating antiferromagnetic phase, and can be rephrased in terms of the hole density $x = 1 - n$ and energy density $e_h(x) = \mathcal{E}(n(x))$.

2.3 Maxwell's construction

In a truly infinite system a phase separation would be associated to a vanishing inverse compressiblity χ^{-1} in the whole density range $n_1 < n < n_2$; in a finite system χ^{-1} may even become negative, because of surface effects; the same applies to the the second derivative of the hole energy density $e_h(x)$ with respect to the hole density x. For finite systems it may be better to pinpoint the phase separation using Maxwell's construction, which is equivalent[20] to studying, as a function of the hole density $x = 1-n$, the quantity $e(x) = [e_h(x)-e_H]/x$. This function is the energy per hole $e_h(x)$ measured relative to its value at half filling $e_H = e_h(x=0)$. For an infinite system, if the inverse compressibility χ^{-1} vanishes between some critical density x_c and half filling $x = 0$, then the function $e(x)$ is a constant for $0 \leq x \leq x_c$, and the fingerprint of a phase separation is a horizontal plot of $e(x)$ below x_c. For a finite system the inverse compressibility χ^{-1} may become negative, and the fingerprint of a phase separation is a minimum[20] of $e(x)$ at $x = x_c$. However even $e(x)$ can give a reliable criterion only for medium-large finite systems; small systems attain too few and coarse densities, and suffer from large finite-size errors.

2.4 Numerical results and pitfalls

Early exact diagonalizations of very small Hubbard clusters[21] are therefore of little use to resolve the question, and even recent fixed-node Green's function Monte Carlo (FNMC)[22] studies of much larger Hubbard lattices[23], although suggestive of the presence of a phase separation for very large $U = 10t$ have shown that further numerical work was needed to settle the problem, mostly because of two reasons. (a) On one hand, the high degeneracy at half filling, which in the "usual" geometry (a square cluster whose sides are parallel to the lattice axes) may result in some sort of artificial phase separation even for lattices as large as 256 sites. (b) On the other hand, the quality of the fixed nodes of the simple Gutzwiller-Slater trial function may significantly depend on the density close to half filling, and again this may result in an artificial phase separation (close to half filling the function $e(x)$ is as sensitive to this error as the second derivative of the energy).

2.5 No charge instabilities

As far as (a) is concerned, an extended cycle of simulations for very large square clusters with tilted sides with respect to the lattice axes has been recently performed for $U = 10t$; the results for the largest lattice (338 sites, or $13\sqrt{2}\times 13\sqrt{2}$) is shown in Fig. 1. Still based on FNMC and simple Gutzwiller-Slater nodes, they seemed to confirm the tendency towards phase separation; the comparison of results before (VMC) and after the fixed-node Green's function projection (FNMC) suggests, however, that the improvement of the wavefunction tends to reduce the phase-separation effect.[24]

As a matter of fact, the problem (b) turns out to be the worse one: according to recent results by Becca, Capone, and Sorella[25], better nodes and a "stochastic reconfiguration" scheme beyond the fixed-node approximation completely wash out the apparent phase separation for small-medium values

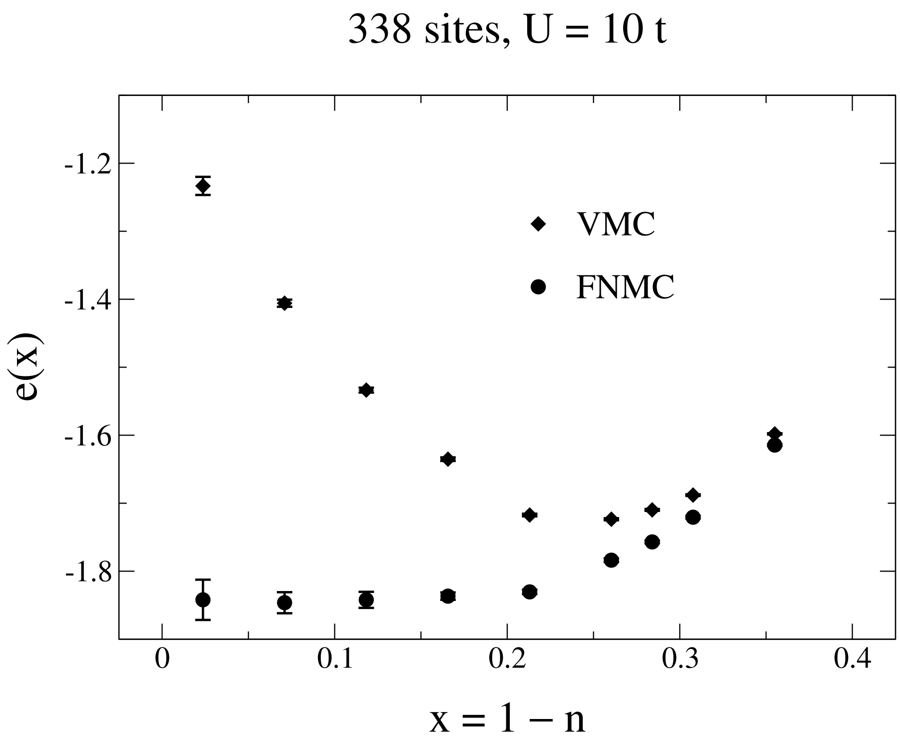

Figure 1. Discrete values of $e(x)$ corresponding to closed-shell densities n plotted against $x = 1-n$ for a 338-site square lattice with 45° tilted sides and periodic boundary conditions, obtained by variational (VMC) and fixed-node Green's function Monte Carlo (FNMC) based on simple Gutzwiller-Slater trial function and nodes. (source: Federico, Cosentini and Bachelet; see text and references).

of the Hubbard $U \leq 4t$; energies vs. density or $e(x)$ functions leave room for some doubts only for $U = 10t$, although, if one insists looking at the energies, the effect appears even less pronounced than our FNMC result of Fig. 1. Their suggestion is to complement the information obtained from the $e(x)$ plots with the study of corresponding correlation functions; this approach seems to rule out phase separation even for the largest values of U/t. Fig. 2 shows this kind of analysis for the case $U = 4t$, but the same is found even for $U = 10t$.[25] This set of calculations seems to conclusively settle a long theoretical controversy, and illustrates well the role of QMC simulations in this type of simple, yet very difficult models of strong correlation; additional effects, not included in

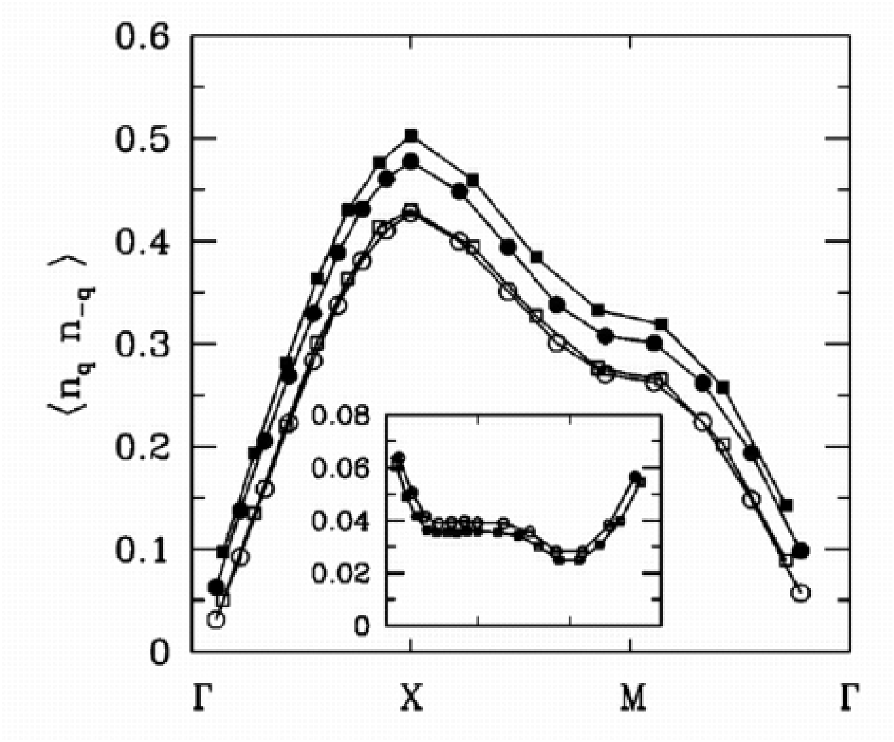

Figure 2. Correlation function for U=4t, 162 electrons on 162 sites (empty circles), 98 electrons on 98 sites (empty squares), 154 electrons on 162 sites (full circles), and 90 electrons on 98 sites (full squares). Lines are guides to the eye and error bars are smaller than points. $\Gamma = (0,0)$ $X = (\pi,\pi)$, $M = (\pi,0)$. In the inset: comparison of the same quantity for the t-J model, $J = 0.6t$ (a situation where the phase separation is proved to occur) for 156 electrons on 162 sites (squares) and 94 electrons on 98 sites (circles). A $q = 0$ peak in the correlation function signals phase separation (t-J, inset); no peak implies no charge instability and thus no phase separation. (source: Becca, Capone and Sorella; see text and references).

this model hamiltonian, must be invoked to explain charge instabilities in cuprate superconductors.

3 Three-dimensional jellium

3.1 The Model

The three-dimensional jellium model consists of N electrons enclosed in a box of volume V (periodically repeated in space) in the presence of a neutralizing background of uniform positive charge density $n^+ = N/V$. The non relativistic jellium is thus governed by the hamiltonian (in Hartree atomic units):

$$H = \sum_{i=1}^{N} \frac{\mathbf{p}_i^2}{2} + \frac{1}{2} \sum_{i \neq j = 1}^{N} \frac{1}{|\mathbf{r}_i - \mathbf{r}_j|} + \Lambda, \tag{2}$$

where Λ represents the effect of the background. The hamiltonian of Eq. (2) describes a model solid whose positive ionic charges are smeared throughout the whole crystal volume to yield a shapeless, uniform positive background (whence the nickname of jellium). When studying this model, one is usually interested in its macroscopic properties, i.e., the thermodynamic limit ($N, V \to \infty$ keeping n constant) of its extensive physical quantities per particle or per volume. Two numbers are enough to describe its zero-temperature phase diagram,[a] namely, the electronic density n and the spin polarization ζ:

$$n = \frac{N}{V} \tag{3}$$

$$\zeta = \frac{|N_\uparrow - N_\downarrow|}{N}, \tag{4}$$

where $N_{\uparrow(\downarrow)}$ is the number of spin-up (down) electrons ($N = N_\uparrow + N_\downarrow$). Instead of the particle density n, it is often convenient to use the Wigner-Seitz radius r_s (in units of the Bohr radius) given by $r_s = \left(\frac{4\pi}{3} n\right)^{-1/3}$; it is also useful to define the Fermi wavevector q_F, simply related to the r_s parameter by $q_F = \left(3\pi^2 n\right)^{1/3} = \left(\frac{9\pi}{4}\right)^{1/3} \frac{1}{r_s}$.

3.2 Jellium as an input for Density Functional Theory

The jellium model represents obviously an unrealistic system. Yet, since the very start of quantum mechanics, it has provided a key conceptual reference and a mine of information for solid-state and many-body theorists.

In the last 35 years, much attention has been devoted to the jellium model because of its relevance in Density Functional Theory (DFT),[2,3] which turns

[a] this only holds for medium and high density; for small density, as predicted by Wigner,[26] the electrons like to crystallize even in the presence of a uniform positive background n^+; the electronic density and spin polarization are no longer uniform in space.

an interacting many-electron system into a noninteracting system subject to an external self-consistent potential. Only one term of this potential, the so-called exchange-correlation energy, is unknown: DFT needs as an input an approximate exchange-correlation energy density functional $E_{xc}[n]$. The results for the uniform electron gas are the basis of the majority of these approximate functionals. This is not surprising since the jellium model, by ignoring the ionic lattice which makes real materials different from one another, allows the theorists to concentrate on key aspects of the electron-electron interaction, which is the hardest part of the many-electron problem.

The correlation energy of jellium as a function of the density r_s and the spin polarization ζ is the basis of the widely used local spin density approximation (LSD). Most of the *abinitio* semilocal and nonlocal exchange-correlation energy density functionals are built up starting from the pair-distribution function of jellium $g(r)$, which is related to the probability of finding two electrons at a distance r from each other. The pair-distribution function of jellium is also the starting point for building up the system-averaged exchange-correlation hole of a system of nonuniform density.[27] The static structure factor $S(q)$ is the Fourier transform of the pair-distribution function. The static local-field $G(q)$ is related to the exchange-correlation kernel and it is also of great interest for DFT.

3.3 The crucial role of Quantum Monte Carlo calculations

Elementary scaling arguments indicate that the kinetic-energy term in Eq. (2) goes as $1/r_s^2$, while the electron-electron Coulomb potential scales as $1/r_s$. Depending on the relative strength between Coulomb and kinetic energies, we can characterize three different regimes: the weak ($r_s \lesssim 1$), intermediate ($1 \lesssim r_s \lesssim 10$), and strong ($r_s \gtrsim 10$) Coulomb coupling regimes.

The random-phase approximation (RPA) provides a rather good description of the weak-coupling regime for the correlation energy, and for the long-range part of $g(r)$. The intermediate coupling region is the one of direct interest for density functional calculations (in real solids the electron density is tipically $1 \lesssim r_s \lesssim 7$). This regime has been widely studied with some approximate physically-motivated semi-analytic schemes,[28,29] which give a good description of most of the physical properties of jellium, but are not accurate enough to provide a powerful tool for the construction of exchange-correlation density functionals. The most reliable results for the quantities relevant for DFT, such as the correlation energy, the pair-distribution function and the static local-field factor are given by the Quantum Monte Carlo simulations.[30,31,32,33,34,35] The strongly-correlated regime is characterized by phase transitions to the fully polarized gas ($\zeta = 1$) and to the Wigner crystal.[26] The most authoritative studies of this region are again provided by the QMC results.[30,35]

Thus, Quantum Monte Carlo simulations provide the most reliable energies of jellium for $1 \lesssim r_s \lesssim 100$, the most reliable pair-distribution functions for the same range of electron densities and for interelectronic distances $0.5 \lesssim r/r_s \lesssim 5$, and the most reliable $S(q)$ and $G(q)$ for relative momentum $0.5 \lesssim q/q_F \lesssim 4$. These regions are unaccessible to exact theories, which tipically work for very high or low densities, and for very small or very large relative momentum q and interelectronic distances r.

3.4 QMC results for the jellium model

Quantum Monte Carlo studies of the 3D jellium model have been carried out with the three main variants of zero-temperature QMC methods for fermion systems: variational Monte Carlo (VMC), fixed-node diffusion Monte Carlo (FN-DMC), and released-node diffusion Monte Carlo (RN-DMC). The studies have been focused on the phase diagram of jellium,[30,35] on the response function,[33] and on the evaluation of the most relevant quantities for density-functional theory, i.e., the correlation energy [30,32,34,35] and the pair-distribution functions.[30,31,32,35] Most of the studies used a Slater-Jastrow trial wavefunctions. The effect of three-body correlations and of the backflow on the total energy has been also investigated.[34] The main uncertainities in the evaluation of the energy is the extrapolation to the infinite system, especially at high densities: QMC simulations are carried out for different total number of particles N, and the results are later extrapolated to the termodynamic limit according to different recipes.

3.5 How to make QMC results available for Density Functional Theory

Quantum Monte Carlo data are available as a finite data set, and for a finite range of electron densities r_s, interelectronic distances r (for the pair-distribution function), or relative momentum q (for the static structure factor and the static local-field factor). To make these data available for use in DFT one needs to provide analytic expressions of the corresponding quantities, i.e. *interpolation* and *extrapolation* are needed. While interpolation can be rather simple, extrapolation is not an easy task. The only way to obtain a reliable extrapolation of QMC data is to make use of as many exact limits as possible for the quantity we want to parametrize. Exact limits usually work in regions unaccessible to QMC simulations. Combining exact analytic properties and QMC data has been the recipe to providing the most reliable results for jellium in the construction of exchange-correlation energy density functionals.

Correlation energy - The RN DMC results of Ceperley and Alder[30] have been the basis of the local-spin-density approximation. The most widely used parametrization of these data are due to Perdew and Zunger[36] (PZ), Vosko, Wilk and Nusair[37] (VWN), and Perdew and Wang[38] (PW). All parametrizations make use of the exact high-density ($r_s \to 0$) and low-density ($r_s \to \infty$) expansions. They also make assumptions on the ζ-dependence to interpolate between $\zeta = 0$ and $\zeta = 1$.

Static local-field factors - The static response of the uniform electron gas with FN DMC has been carried out by Moroni, Ceperley and Senatore.[33] Their results have been parametrized by Corradini *et al.*[39], again including most of the known exact limits for the static local-field factor $G(q)$. Alternative expressions for the same quantity can be obtained by using the QMC data for the pair-distribution function and then applying the Singwi-Tosi-Land-Sjölander[29] (STLS) scheme to obtain the local-field factor. The STLS is an approximation and so it gives raise to an approximate $G(q)$. Analytic expressions for the local-field factor obtained in this way can be found in Refs. [40] and [41], which also includes the magnetic local-field factor.

Pair-distribution functions and static structure factors - A first calculation of the pair-distribution functions of jellium with DMC was performed by Ceperley and Alder.[30] Perdew and Wang[42] built up an analytic model for $g(r)$, in which the QMC data were used only for optimizing the ζ-dependence. No information from QMC results about the r or r_s dependence was used. In real space, the Perdew-Wang model is in reasonable agreement with QMC data for small r_s. Its spin-resolved version does not perform very well, especially in reciprocal space.[43] A recent extensive study of the spin-resolved pair-distribution functions and static structure factors with FN DMC has been carried out by Ortiz and Ballone,[32] and by Ortiz, Harris and Ballone.[35] Their data have been parametrized by Gori-Giorgi, Sacchetti and Bachelet[43] (GSB), using functional forms which are analytic and closed-form both in real and reciprocal space, and include some new properties. As an example, in Fig. 3 is reported the pair-distribution function for different values of the electron density. Both the DMC data by Ortiz, Harris and Ballone[35] and the analytic parametrization thereof by Gori-Giorgi, Sacchetti and Bachelet[43] are shown. The GSB approach also allows to extract from QMC simulations the spin-resolved correlation energies. The inclusion of the new properties written down by Gori-Giorgi, Sacchetti and Bachelet in the Perdew-Wang model fairly improves its agreement with QMC data in reciprocal space.[44]

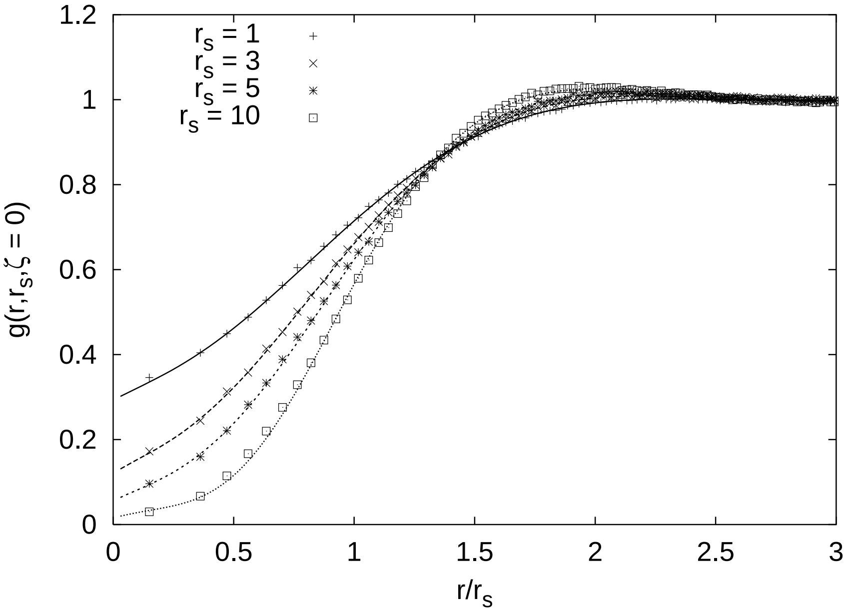

Figure 3. Diffusion Monte Carlo of the pair-distribution function of jellium[35] for different values of the electron density. Also shown is the analytic parametrization thereof by Gori-Giorgi, Sacchetti and Bachelet[43] (solid, dashed, short-dashed and dotted lines).

Acknowledgments

GBB and PGG acknowledge partial financial support from MURST (the Italian Ministry for University, Research and Technology) through COFIN99.

References

1. W. M. C. Foulkes, L. Mitáš, R. J. Needs, G. Rajagopal, *Rev. Mod. Phys.* **73**, 33 (2001).
2. P. Hohenberg and W. Kohn, *Phys. Rev.* **136**, B864 (1964).
3. W. Kohn and L. J. Sham, *Phys. Rev.* **140**, A1133 (1965).
4. see also W. Kohn, *Rev. Mod. Phys.* **71**, 1253 (1999).
5. see e.g. J. P. Perdew, K. Burke, and M. Ernzerhof, *Phys. Rev. Lett.* **77**, 3865 (1996); (E) **78**, 1396 (1997).
6. D. R. Hamann, M. Schlüter, and C. Chiang, *Phys. Rev. Lett.* **43**, 1494

(1979).
7. R. Car and M. Parrinello, *Phys. Rev. Lett.* **55**, 2471 (1985).
8. S. Baroni, P. Giannozzi, and A. Testa, *Phys. Rev. Lett.* **59**, 2662 (1987).
9. see e.g. the ABINIT public-domain programs and web site.
10. see e.g. M. Boero, M. Parrinello, and K. Terakura, J. Am. Chem. Soc. **120**, 2746 (1998).
11. S. Y. Savrasov, G. Kotliar, and E. Abrahams, Nature **410**, 793 (2001).
12. A. Malatesta, S. B. Fahy, and G. B.Bachelet, *Phys. Rev.* B **56**, 12201 (1997), and refs. therein.
13. C. Filippi, C. J. Umrigar, and X. Gonze, *Phys. Rev.* A **45**, 4810 (1996); *Theoretical and Computational Chemistry: Recent Developments in Density Functional Theory*, edited by J. Seminario (Elsevier Publisher, 1996)
14. G. B. Bachelet, D. M. Ceperley, and M. Chiocchetti, *Phys. Rev. Lett.* **62**, 2088 (1989).
15. Y. Lee, P. R. C. Kent, M. D. Towler, R. J. Needs, and G. Rajagopal PRB **62**, 13347 (2000).
16. D. Bressanini, P. J. Reynolds, and D. M. Ceperley, this volume.
17. C. J. Umrigar and C. Filippi, this volume; D. M. Ceperley, this volume.
18. M. Grilli, R. Raimondi, C. Castellani, C. Di Castro, and G. Kotliar, *Phys. Rev. Lett.* **67**, 259 (1991); C. Di Castro, and M. Grilli Physica Scripta **T45**, 81 (1992), and refs. therein.
19. V. J. Emery and S. A. Kivelson Physica C **209**, 597 (1993).
20. V. J. Emery, S. A. Kivelson, and H. Q. Lin, *Phys. Rev. Lett.* **64**, 475 (1990).
21. E. Dagotto, A. Moreo, F. Ortolani, D. Poilblanc, and J. Riera, *Phys. Rev.* B **45**, 10741 (1992).
22. H. J. M. van Bemmel, D. F. B. ten Haaf, W. van Saarloos, J. M. J. van Leeuwen, and G. An, *Phys. Rev. Lett.* **72**, 1442 (1994); D. F. B. ten Haaf, H. J. M. van Bemmel, J. M. J. van Leeuwen, W. van Saarloos, and D. M. Ceperley, *Phys. Rev.* B **51**, 13039 (1995).
23. A.C. Cosentini, M. Capone, L. Guidoni, and G. B. Bachelet, *Phys. Rev.* B **58**, R14685 (1998); G.B. Bachelet and A. Cosentini, in: *Quantum Monte Carlo in Physics and Chemistry* (C. Umrigar and M. P. Nightingale, Eds.), p. 375-397, NATO-ASI series, Kluwer Academic Publishers, Dordrecht (1999).
24. A. Federico, A.C. Cosentini, and G. B. Bachelet, unpublished (2000).
25. F. Becca, M. Capone,and S. Sorella *Phys. Rev.* B **62**, 12700 (2000).
26. E. Wigner, *Phys. Rev.* **46**, 1002 (1934).
27. J. P. Perdew, K. Burke, and Y. Wang, *Phys. Rev.* B **54**, 16533 (1996).
28. K. S. Singwi and M. P.Tosi, *Solid State Physics* **36**, 177 (1981).

29. K. S. Singwi, M. P.Tosi, R. H. Land, and A. Sjölander, *Phys. Rev.* **176**, 589 (1968).
30. D. M. Ceperley and B. J. Alder, *Phys. Rev. Lett.* **45**, 566 (1980).
31. W. E. Pickett and J. Q. Broughton, *Phys. Rev.* B **48**, 14859 (1993).
32. G. Ortiz and P. Ballone, *Phys. Rev.* B **50**, 1391 (1994); **56**, 9970 (1997).
33. S. Moroni, D. M. Ceperley, and G. Senatore, *Phys. Rev. Lett.* **69**, 1837 (1992); **75**, 826 (1995).
34. Y. Kwon, D. M. Ceperley, and R. M. Martin, *Phys. Rev.* B **58**, 6800 (1998).
35. G. Ortiz, M. Harris, and P. Ballone, *Phys. Rev. Lett.* **82**, 5317 (1999).
36. J. P. Perdew and A. Zunger, *Phys. Rev.* B **23**, 5048 (1981).
37. S. H. Vosko, L. Wilk, and M. Nusair, *Can. J. Phys.* **58**, 1200 (1980).
38. J. P. Perdew and Y. Wang, *Phys. Rev.* B **45**, 13244 (1992).
39. M. Corradini, R. Del Sole, G. Onida, and M. Palummo, *Phys. Rev.* B **57**, 14569 (1998).
40. J. L. Bretonnet and M. Boulahbak, *Phys. Rev.* B **53**, 6859 (1996).
41. G. B. Bachelet, P. Gori-Giorgi, and F. Sacchetti, in *Density Functional Theory and Its Applications to Materials*, edited by V. E. Van Doren, K. Van Alsenoy, and P. Geerlings (AIP 2001), to appear.
42. J. P. Perdew and Y. Wang, *Phys. Rev.* B **46**, 12947 (1992); **56**, 7018 (1997).
43. P. Gori-Giorgi, F. Sacchetti, and G. B. Bachelet, *Phys. Rev.* B **61**, 7353 (2000).
44. K. Schmidt, S. Kurth, J. Tao, and J. P. Perdew, *Phys. Rev.* B **62**, 2227 (2000).